A NUMERICAL ANALYSIS ON THE AERODYNAMIC NOISE OF CROSS-FLOW FAN BY USING A 2-D URANS SIMULATION AND ACOUSTIC ANALOGY

Myungsung LEE, Seongwon KANG, Nahmkeon HUR

Department of Mechanical Engineering, Sogang University, Seoul, Korea

SUMMARY

The aerodynamic noise of a cross-flow fan in an air-conditioner was investigated by using 2-D compressible URANS simulation and FW-H acoustic analogy. The pressure fluctuations on the fan blades and casing walls obtained from the 2-D CFD simulation were used as input values in the FW-H acoustic analysis. The CFD results showed the typical flow field of the cross-flow fan including an eccentric vortex which was strongly correlated with the fan performance. To validate the present numerical methods, the spectral sound pressure level (SPL) was compared with available experimental data, and the predicted overall SPL spectrum was in a good agreement with the experiment. The noise contributions of each component in the air-conditioner on the overall SPL spectrum were also discussed. The results of the present study could be used for the optimal design of air-conditioner to reduce the aerodynamic noise due to cross-flow fan.

INTRODUCTION

Recently, public interest has been rising not only in the high performance and efficiency of an air-conditioner (AC) but also the noise problem of AC. The cross-flow fan (CFF), which is commonly used in the AC, is the dominant cause of the noise problem among others. The aerodynamic noise due to the CFF can be divided into the tonal and broadband noise. The tonal noise is induced by the periodic interactions between the rotating blades and stationary casing walls such as the stabilizer and rear guider, while the broadband noise is generated due to the random flow characteristic like turbulent fluctuation.

In earlier works, many experimental studies [1-5] have showed that geometries of the casing walls and flow coefficient strongly affect the overall performance and noise emission of the CFF. In particular, Lazzaretto et al. [3] and Toffolo et al. [4] showed the effects of important geometric parameters on the overall performance of CFF and established the guidelines for the optimized design of fan casing. Flow visualization studies were also performed based on the smoke-stream method by Tsai et al. [6] who provided a qualitative description of the flow field of a CFF. However,

the experimental studies have inherent limitations that only low spatial resolution measurements are allowed and the whole inner region of CFF cannot be covered.

More recently, Computational Fluid Dynamics (CFD) studies have been carried out by several researchers [7-12] for the numerical simulations to investigate the flow field and aerodynamic noise of the CFF. Compared to the broadband noise of CFF, the tonal noise has obvious noise peaks which are very annoying to the human ear, especially at the blade passing frequency (BPF). For this reason, much effort has been devoted to reduce the BPF tonal noise, which can be divided into two aspects: (i) modify the location and shape of the stabilizer. Koo [7] reduced the tonal noise at the BPF by using skewed stabilizer along spanwise direction. (ii) Modify the impeller geometry. Other numerical studies [8,9] indicate that a well-designed random pitched impeller can modulate the BPF tonal noise and its harmonics into series of relatively small noise peaks. However, these previous CFD studies have provided only qualitative predictions, and quantitative comparisons of the noise prediction with experimental data have not been sufficiently conducted.

In the present study, the aerodynamic noise characteristics of CFF in AC indoor unit (IDU) were numerically investigated and quantitatively compared with available experimental data in various operating conditions of CFF. The flow field of CFF was obtained by solving the 2-D compressible Reynolds-Averaged Navier-Stokes (RANS) equation to capture the acoustic wave generated in the AC IDU. The rigid body motion technique was adopted to consider the rotating motion of CFF at the arbitrary sliding interface (ASI) between the region rotating with fan blades and other stationary region. The propagated acoustic pressure toward a microphone was computed by using the Ffowcs Williams-Hawkings (FW-H) acoustic analogy equation. The results of the present study can be expected to provide useful information for the low noise design of AC IDU.

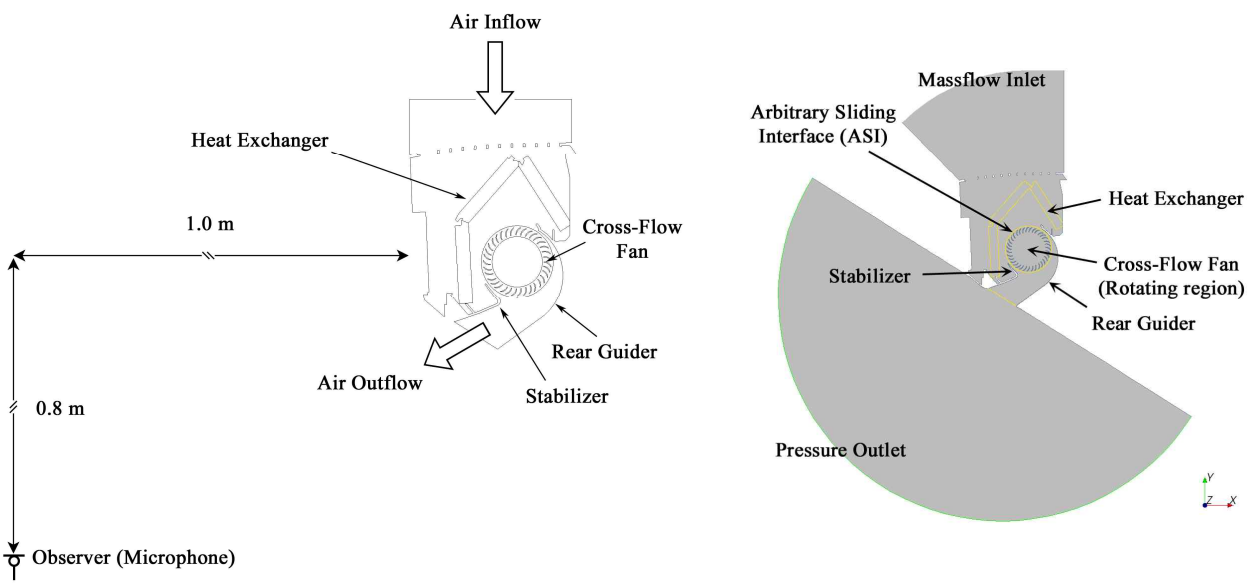

Figure 1: Cross-sectional view of the considered cross-flow fan in air-conditioner indoor unit with the location of the microphone to measure aerodynamic noise (left) and 2-D computational domain consisting of rotating and stationary regions (right)

NUMERICAL METHODS

For simulating the unsteady flow field due to the rotating CFF in AC IDU, the 2-D compressible Reynolds-averaged continuity, momentum and energy equations were solved:

$$\frac{\partial \rho}{\partial t}+\frac{\partial(\rho u_i)}{\partial x_i}=0 \tag{1}$$

$$\frac{\partial(\rho u_i)}{\partial t}+\frac{\partial(\rho u_i u_j)}{\partial x_j}=-\frac{\partial p}{\partial x_i}+\frac{\partial \sigma_{ij}}{\partial x_j}+\frac{\partial \tau_{ij}}{\partial x_j} \tag{2}$$

$$c_p\left[\frac{\partial(\rho T)}{\partial t}+\frac{\partial(\rho u_i T)}{\partial x_i}\right]=\frac{\partial p}{\partial t}+u_i\frac{\partial p}{\partial x_i}-\frac{\partial \dot{q}_i}{\partial x_i}+(\sigma_{ij}+\tau_{ij})\frac{\partial u_j}{\partial x_i} \tag{3}$$

$$p=\rho RT \tag{4}$$

where σ_{ij} and τ_{ij} are the viscous stress tensor and Reynolds stress tensor. The viscous and Reynolds stresses are defined as:

$$\sigma_{ij}=2\mu S_{ij} \tag{5}$$

$$\tau_{ij}=-\rho\overline{u'_j u'_i} \tag{6}$$

where S_{ij} is the strain rate tensor:

$$S_{ij}=\frac{1}{2}\left(\frac{\partial u_i}{\partial x_j}+\frac{\partial u_j}{\partial x_i}\right) \tag{7}$$

The heat flux $\dot{q}_i$ in the energy equation is defined with temperature gradient:

$$\dot{q}_i=c_p\frac{\mu}{\Pr}\frac{\partial T}{\partial x_i} \tag{8}$$

The results of CFD simulation were used as the input values for an acoustic analogy model. For the acoustic analogy analysis, the Ffowcs Williams-Hawkings (FW-H) equation was used. The FW-H formulation considered in the present study is based on the Farassat's Formulation 1A, which is the non-convective form of the FW-H equation [13].

The FW-H equation is an exact rearrangement of the continuity and the momentum equations into the form of an inhomogeneous wave equation, which is based on the free-space Green's function to compute the sound pressure p' at the observer location, $\mathbf{x}$. Using FW-H equation, the sound pressure at observer can be computed by summing the contributions of all noise source elements:

$$p'(\mathbf{x},t)=\sum_{i=1}^{n_s}\left[p'_{t,i}(\mathbf{x},t)+p'_{l,i}(\mathbf{x},t)\right] \tag{9}$$

where $\mathbf{x}$ is a position vector to the observer and t is an observer time. In the right side of equation, the first term p'_t is monopole term, also known as the thickness source, resulting from the displacement of fluid as the body passes. The second term p'_l is dipole term, also known as the loading source; this models the noise generated by the transient motion of the force distribution on the body surface e.g. loading noise, blade-vortex interaction noise and broadband noise. Each term can be written as:

$$4\pi p'_{t,i}(\mathbf{x},t)=\left[\frac{\rho_0(\dot{U}_n+U_{\dot{n}})}{r_i(1-M_r)^2}\right]_{ret}+\left[\frac{\rho_0 U_n\left[r_i\dot{M}_r+c_0(M_r-M^2)\right]}{r_i^2(1-M_r)^3}\right]_{ret} \tag{10}$$

$$4\pi p'_{l,i}(\mathbf{x},t)=\frac{1}{c_0}\left[\frac{\dot{L}_r}{r_i(1-M_r)^2}\right]_{ret}+\left[\frac{(L_r-L_M)}{r_i^2(1-M_r)^2}\right]_{ret}+\frac{1}{c_0}\left[\frac{L_r\left[r_i\dot{M}_r+c_0\left(M_r-M^2\right)\right]}{r_i^2(1-M_r)^3}\right]_{ret} \tag{11}$$

where r_i is a position vector from the noise source $\mathbf{y}_i$ to the observer $\mathbf{x}$:

$$r_i=\mathbf{x}-\mathbf{y}_i \tag{12}$$

and:

$$\mathbf{U}_i=\mathbf{v}_i+\frac{\rho}{\rho_0}(\mathbf{u}_i-\mathbf{v}_i),\quad \dot{\mathbf{U}}_i=\frac{\partial\mathbf{U}_i}{\partial\tau},\quad U_n=\mathbf{n}_i\bullet\mathbf{U}_i,\quad \dot{U}_n=\mathbf{n}_i\bullet\frac{\partial\mathbf{U}_i}{\partial\tau},\quad U_{\dot{n}}=\frac{\partial\mathbf{n}_i}{\partial\tau}\bullet\mathbf{U}_i \tag{13}$$

$$\mathbf{M}_i=\frac{\mathbf{v}_i}{c_0}=\frac{1}{c_0}\frac{\partial\mathbf{y}_i}{\partial\tau},\quad M^2=\mathbf{M}_i\bullet\mathbf{M}_i,\quad \dot{\mathbf{M}}_i=\frac{\partial\mathbf{M}_i}{\partial\tau}=\frac{1}{c_0}\frac{\partial^2\mathbf{y}_i}{\partial\tau^2},\quad M_r=\mathbf{r}_i\bullet\mathbf{M}_i,\quad \dot{M}_r=\mathbf{r}_i\bullet\frac{\partial\mathbf{M}_i}{\partial\tau} \tag{14}$$

$$\mathbf{L}_i=\mathbf{P}_{ij}\mathbf{n}_j+\frac{\rho}{u_i}(u_n-v_n),\quad \dot{\mathbf{L}}_i=\frac{\partial\mathbf{L}_i}{\partial\tau},\quad L_r=\mathbf{r}_i\bullet\mathbf{L}_i,\quad \dot{L}_r=\mathbf{r}_i\bullet\frac{\partial\mathbf{L}_i}{\partial\tau},\quad L_M=\mathbf{M}_i\bullet\mathbf{L}_i \tag{15}$$

where $\mathbf{u}_i$ represents fluid velocity components in the x_i direction, u_n the fluid velocity component normal to the body surface, $\mathbf{v}_i$ the surface velocity components in the x_i direction, v_n the surface velocity component normal to the surface. $\mathbf{n}_i$ is the unit normal vector pointing from the surface toward the exterior region. $\mathbf{r}_i$ is the unit vector from noise source to the observer

$$\mathbf{r}_i=\frac{\mathbf{x}-\mathbf{y}_i}{|r_i|} \tag{16}$$

The terms in the brackets were evaluated at a retarded time τ which is defined as:

$$\tau=t-\frac{r_i(\tau)}{c_0} \tag{17}$$

The crucial part of the FW-H analysis is how to account for the time-lag between emission and reception times. To computed the acoustic pressure $p'(\mathbf{x},t)$, first calculate the monopole and dipole noise sources generated at the retarded time τ, second determine the distance $r_i(t)$ between the source element and observer, then compute the observer time t, finally sort the acoustic pressure with respect to the arrival times at the observer after the sound pressure are known at each instantaneous retarded time τ. A sound pressure level (SPL) was computed by

$$\mathrm{SPL}=10\log_{10}\left(\frac{p'_{rms}}{p_{ref}}\right)^2 \tag{18}$$

where p'_{rms} is a root mean square of the acoustic pressure and $p_{ref}\,(=20\ \mu\mathrm{Pa})$ is a reference pressure. The SPL spectrum was obtained by Fourier transform algorithm.

The AC IDU considered in the present study is illustrated in the left of Fig. 1. The components of the AC IDU are CFF, stabilizer, rear guider, heat exchanger, etc. In the experiment, the microphone was used to measure the far field noise as shown in the figure. Since the geometry of the CFF is symmetric in the span direction, 2-D domain was considered in the present study. The total 2-D computational domain is shown in the right of Fig. 1, which consists of the AC IDU, upside and downside chambers. Fixed mass flow rate was applied at the inlet boundary condition, which was obtained from the experiment. The atmospheric pressure condition was adopted at the outflow boundary.

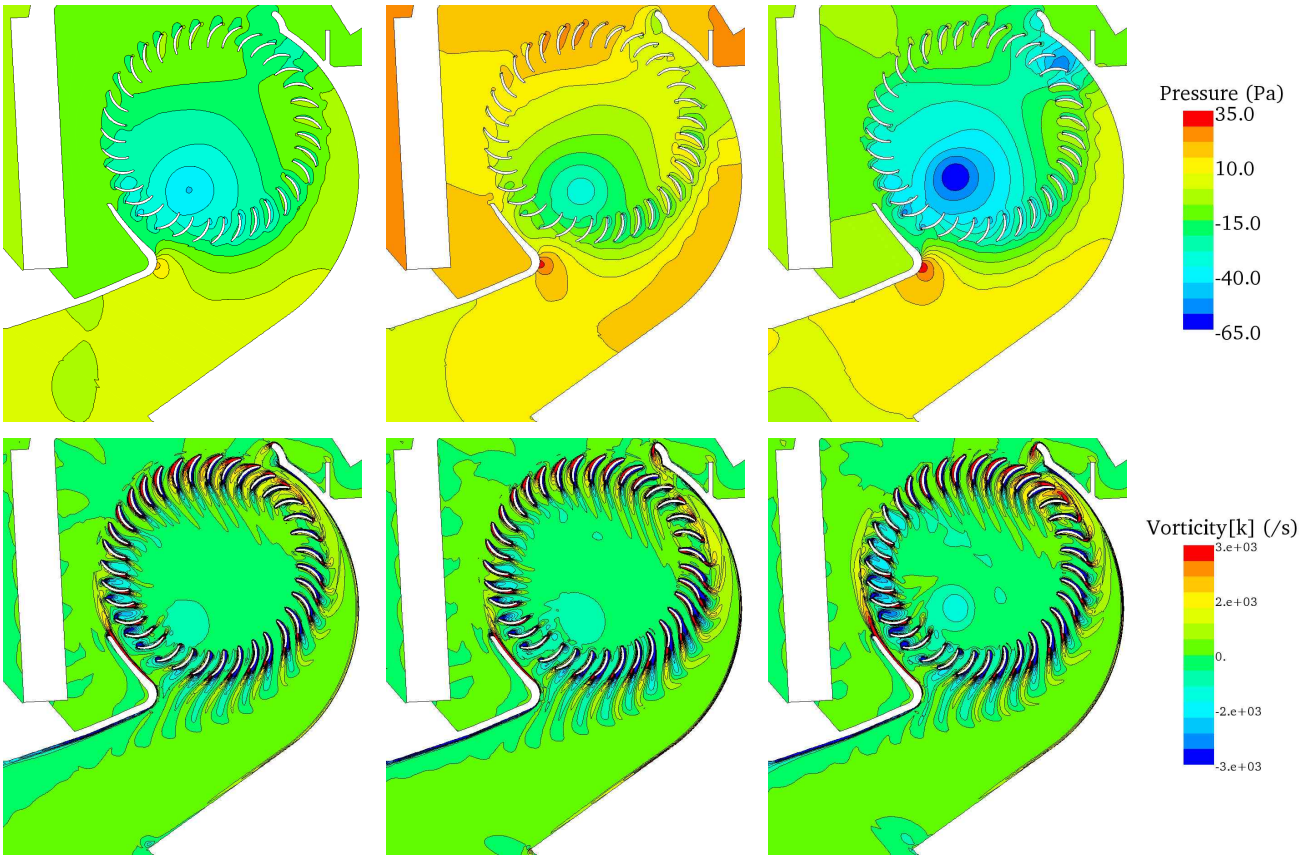

(a) 877 rpm *(b) 998 rpm* *(c) 1129.5 rpm*

Figure 2: Instantaneous flow field predicted by 2-D URANS with variation of the rotating speed of cross-flow fan: pressure (up) and vorticity (down) distributions

The whole computational domain can be divided into rotating and stationary regions. The sliding interface for the rigid body motion method was adopted between the two regions. To consider the rotating motion of the CFF, the mesh block containing the fan blades was moving along the sliding interface. The pressure drop through the heat exchanger region was considered by using the porous media model to replace the complex geometry of louver fin in the heat exchanger with simple computational mesh. A relation between pressure drop and velocity magnitude was obtained from experiment. In the present study, three operating conditions of the CFF were considered: 877, 998, 1129.5 rpm. Total 222,000 computational cells were used in the 2-D domain. STAR-CCM+ V6.04.016 [14] was employed to simulate the flow field of CFF in the AC IDU. Transient compressible 2-D Navier-Stokes equation was solved with standard k-ε model for turbulence. For the simulation, a 4-CPU Linux cluster with Intel Xeon Quad-Core E5620 2.4 GHz 64-bit processor was used to perform the parallel computation. The computation time was around 30 hours for 1 revolution of CFF.

RESULTS AND DISCUSSION

To obtain the transient wall pressure fluctuation of the fan blades, stabilizer and rear guider, CFD simulations were conducted. Fig. 2 shows the instantaneous flow field predicted from 2-D URANS simulations with various rotating speed of CFF. The result showed the typical flow field of CFF such as an off-centered vortex flow in the vicinity of the stabilizer, which is known as the eccentric vortex. It is also known that the location of center of the eccentric vortex so-called vortex eye is

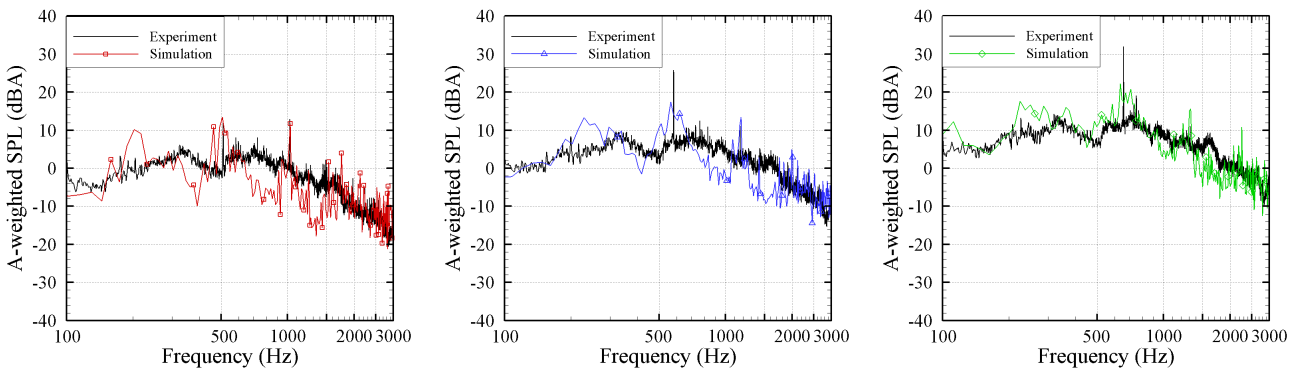

(a) 877 rpm *(b) 998 rpm* *(c) 1129.5 rpm*

Figure 3: Time history of the acoustic pressure at microphone predicted by FW-H analysis with variation of rotating speed of cross-flow fan (up) and comparison of the spectral sound pressure level (SPL) with experimental measurement (down)

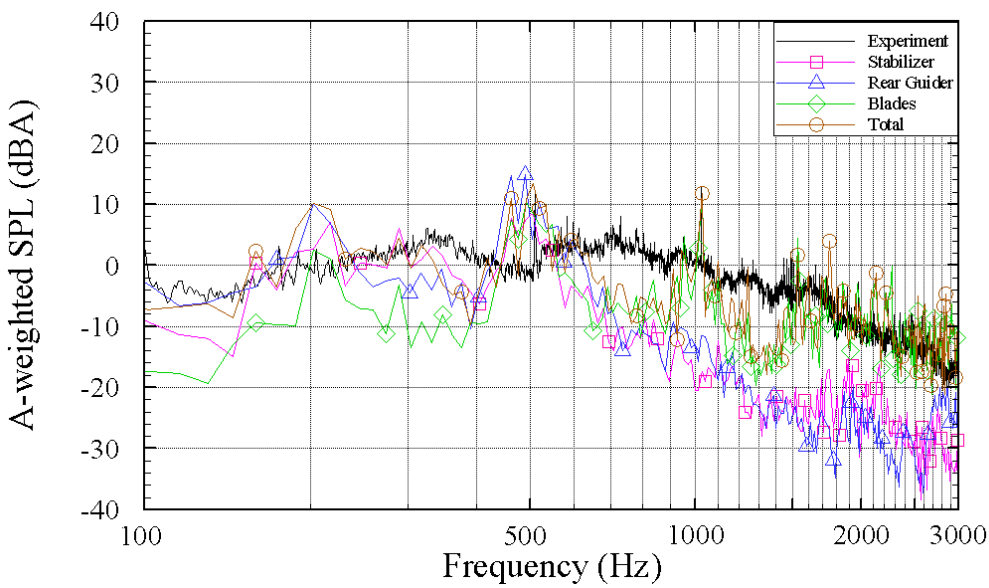

Figure 4: Contribution of each component in the air-conditioner such as stabilizer, rear guider and blades on the overall SPL spectrum in case of 877 rpm

strongly correlated with the flow rate; as the vortex eye is located close to the stabilizer, the flow rate is increased due to the reduction of recirculation region around the vortex eye. From the results of the present study, the vortex eye was found in the vicinity of the stabilizer in all cases. The maximum negative pressure was appeared at the vortex eye, and the maximum negative pressure was increased with the rotating speed of CFF as shown in figure. It was noted that the negative pressure was also found in the vicinity of the rear guider; this is due to the highly flow separation generated as the air flows by the narrow region between blade and rear guider so-called the nozzle of rear guider. On the other hand, the maximum positive pressure was predicted where the blade wake was impinged upon the stabilizer. The maximum positive pressure also became higher as the rotating speed of CFF was increased.

The transient pressure fluctuation obtained from 2-D CFD simulations was used as the input values for the FW-H acoustic analogy analysis to compute the far-field noise at the microphone. The horizontal and vertical distances from the air-conditioner to the microphone were 1.0 m and 0.8 m,

respectively. The numerical acoustic predictions of SPL at the microphone were obtained by computing the surface integral on solid surfaces of stabilizer, rear guider and 35 blades. Fig. 3 shows the acoustic results predicted by the FW-H acoustic analysis. The far field noise of CFF is computed during 54,000 time steps, i.e. 9 revolutions of CFF. The spectral results were obtained by averaging 5 Fourier transforms with overlap factor 0.1 and Hanning window, which led to a spectral resolution of $\Delta f \sim 15$ Hz. The spectral resolution of the Fourier transforms can be improved as the number of data of the predicted acoustic pressure is increased. To compare the computed spectral results to the experimental data, both numerical prediction and experiment measurement were converted to the A-weighted SPL.

The predicted spectral A-weighted SPL was compared with experimental data as shown in Fig. 3. Globally, the results of the present study are in good agreement with the experimental measurement in the whole spectrum. In the case of 877 rpm, the peak SPL at BPF was predicted accurately compared to the experimental one, while the peak SPL in cases of 998 and 1129.5 rpm were underestimated than the experiment about 8 dBA. The discrepancy in these two cases might be due to the fact that the grid size and time step are the same in all cases. For this reason, the number of time step required for one revolution of CFF in the cases of 998 and 1129.5 rpm were smaller than that of 877 rpm case. To overcome this, the sensitivities of the grid density and time step for various operating conditions of CFF would be evaluated.

Fig. 4 shows the noise contributions due to the stabilizer, rear guider and blades, separately in the case of 877 rpm. The pink, blue and green lines in the figure represent the noise contributions of the stabilizer, rear guider and blades, respectively. The brown line represents the noise contribution due to total integration surface consisting of stabilizer, rear guider and blades. The relative contribution of each FW-H integration surface breaks down as follows: below 200 Hz the rear guider dominates, between 200 and 500 Hz the stabilizer contributes more than the rear guider, and between 500 and 800 Hz noise contributions due to the stabilizer, rear guider and blades are of the same order, and above 800 Hz the blades dominate.

CONCLUDING REMARKS

In the present study, the aerodynamic noise generated by the cross-flow fan inside an air-conditioner indoor unit was investigated with the URANS simulation and acoustic analogy theory. Since the flow field of the cross-flow fan was assumed to be strongly correlated in the axial direction, 2-D CFD simulations were conducted. Considering the rotating motion of the cross flow fan, the rigid body motion technique was used to rotate the mesh block containing the fan blades. The turbulent flow was predicted with the standard k-ε model. The CFD results showed the typical flow field of cross-flow fan including the eccentric vortex. In various operating conditions, the maximum negative pressure predicted at the vortex eye became higher as the rotating speed of cross-flow fan was increased. Using the CFD results such as the pressure fluctuation on the surface of fan blades, stabilizer, and rear guider, the sound pressure level (SPL) at the microphone was computed by the FW-H acoustic analogy. The overall SPL spectrum predicted by using the FW-H was in good agreement with the experiment. The results of the present study, therefore, can be used for the optimal design of the components of air-conditioner to reduce the aerodynamic noise. In the future study, the accuracy of the numerical result would be enhanced by adopting DES and LES.

ACKNOWLEDGMENT

This work was supported by the National Research Foundation of Korea (NRF) grant No. 20090083510 funded by the Korean government (MEST) through Multi-phenomena CFD Engineering Research Center (ERC).

BIBLIOGRAPHY

[1] L. Lazzarotto, A. Lazzaretto, A. D. Martegani, A. Macor – *On cross-flow fan similarity: effects of casing shape*. Journal of Fluids Engineering 123(3), 523-531, **2001**

[2] A. Lazzaretto – *A criterion to define cross-flow fan design parameters*. Journal of Fluids Engineering 125(4), 680-683, **2003**

[3] A. Lazzaretto, A. Toffolo, A. D. Martegani – *A systematic experimental approach to cross-flow fan design*. Journal of Fluids Engineering 125(4), 684−693, **2003**

[4] A. Toffolo, A. Lazzaretto, A. D. Martegani – *An experimental investigation of the flow field pattern within the impeller of a cross-flow fan*. Experimental Thermal and Fluid Science 29(1), 53−64, **2004**

[5] A. Toffolo, A. Lazzaretto, A. D. Martegani – *Cross-flow fan design guidelines for multi-objective performance optimization*. Journal of Power and Energy 218, 33−42, **2004**

[6] G.-L. Tsai, T.-H. Tu, T.-C. Li, K.-H. Wang – *Flow style investigation and noise reduction of a cross-flow fan with varied rotor-skew-angle rotor*. JSME International Journal Series B 49(3), 695−704, **2006**

[7] H. M. Koo – *Discrete frequency noise reduction of the cross-flow fan of the split type room air-conditioners using the skewed stabilizers*. JSME International Journal Series C 43(1), 104−109, **2000**

[8] Y. Cho, Y. J. Moon – *Discrete noise prediction of variable pitch cross-flow fans by unsteady Navier-Stokes computations*. Journal of Fluids Engineering 125(3), 543−550, **2003**

[9] Y. J. Moon, Y. Cho, H. S. Nam – *Computational of unsteady viscous flow and aeroacoustic noise of cross flow fans*. Computers & Fluids, 32(7), 995−1015, **2003**

[10] M. Gabi, T. Klemm – *Numerical and experimental investigations of cross-flow fans*. Journal of Computational and Applied Mechanics 5(2), 251−261, **2004**

[11] A. Toffolo – *On the theoretical link between design parameters and performance in cross-flow fans: a numerical and experimental study*. Computers & Fluids 34(1), 49−66, **2005**

[12] Y. Li, H. Ouyang, J. Tian, Z. Du, Z. Zheng – *Experimental and numerical studies on the discrete noise about the cross-flow fan with block-shifted impellers*. Applied Acoustics 71(12), 1142−1155, **2010**

[13] F. Farassat – *Derivation of formulations 1 and 1A of Farassat*. NASA, TM-2007-214853, **2007**

[14] CD-adapco Group – *STAR-CCM+ Version 6.04.016 USER GUIDE*, **2011**

© Myungsung Lee, Seongwon Kang, Nahmkeon Hur